

Research article

Removal of atmospheric CO₂ by engineered soils in infrastructure projectsM. Ehsan Jorat^{a,b,*}, Karl E. Kraavi^b, David A.C. Manning^b^a School of Applied Sciences, Abertay University, United Kingdom^b School of Natural & Environmental Sciences, Newcastle University, United Kingdom

ARTICLE INFO

Keywords:

Urban land
Carbon sequestration
Carbon precipitation
Geotechnical investigation
Environmental impact
Isotope analysis

ABSTRACT

The use of crushed basic igneous rock and crushed concrete for enhanced rock weathering and to facilitate pedogenic carbonate precipitation provides a promising method of carbon sequestration. However, many of the controls on precipitation and subsequent effects on soil properties remain poorly understood. In this study, engineered soil plots, with different ratios of concrete or dolerite combined with sand, have been used to investigate relationships between sequestered inorganic carbon and geotechnical properties, over a two-year period. Cone penetration tests with porewater pressure measurements (CPTu) were conducted to determine changes in tip resistance and pore pressure. C and O isotope analysis was carried out to confirm the pedogenic origin of carbonate minerals. TIC analysis shows greater precipitation of pedogenic carbonate in plots containing concrete than those with dolerite, with the highest sequestration values of plots containing each material being equivalent to 33.7 t C ha⁻¹ yr⁻¹ and 17.5 t C ha⁻¹ yr⁻¹, respectively, calculated from extrapolation of results derived from the TIC analysis. TIC content showed reduction or remained unchanged for the top 0.1 m of soil; at a depth of 0.2 m however, for dolerite plots, a pattern of seasonal accumulation and loss of TIC emerged. CPTu tip resistance measurements showed that the presence of carbonates had no observable effect on penetration resistance, and in the case of porewater pressure measurements, carbonate precipitation does not change the permeability of the substrate, and so does not affect drainage. The results of this study indicate that both the addition of dolerite and concrete serve to enhance CO₂ removal in soils, that soil temperature appears to be a control on TIC precipitation, and that mineral carbonation in constructed soils does not lead to reduced drainage or an increased risk of flooding.

1. Introduction

The rise in atmospheric CO₂ concentration is the key driver of climate change (Friedlingstein et al., 2020). Annual carbon fluxes to the atmosphere from fossil fuel combustion in 2019 were 9.9 Gt C yr⁻¹ and 1.8 Gt C yr⁻¹ from landuse change, giving a total net anthropogenic contribution (which takes into account cement carbonation) of 11.5 Gt C yr⁻¹ emitted annually, which sinks to the ocean and land at the rate of 2.6 and 3.1 Gt C yr⁻¹, respectively (Friedlingstein et al., 2020). The challenge of reducing CO₂ emissions from fossil fuel combustion needs to be augmented by removal of CO₂ from the atmosphere in order to achieve goals that reduce the risk of catastrophic climate change. One such approach is to retain CO₂ removed by photosynthesis in soils and hydrological/hydrogeological systems as inorganic C (bicarbonate in solution or carbonate minerals; Beerling et al., 2020; Manning et al., 2013), thus removing carbon from the biological cycle. Globally, Renforth et al. (2011) recognise the significance of using soil processes to

remove atmospheric CO₂, given that soil represents a carbon pool of up to 1500 Gt C which is twice that of the atmosphere (730 Gt C).

Removal of carbon from the biological carbon cycle involves two processes: carbonation (i.e. the formation of pedogenic carbonate minerals in soils; Manning et al., 2013) and enhanced rock weathering (ERW; Beerling et al., 2020; Haque et al., 2020; Haque et al., 2021; Khalidy et al., 2021). For ERW, the focus has been application of Ca and Mg silicate rocks, as rock dust or 'fines', to agricultural soils, given their large area and scope for adopting the approach globally (e.g., Kelland et al., 2020). However, even at application rates of 100 t ha⁻¹ (well above current recommended rates for rock dust use in agriculture, and typically corresponding to removal of 23 t CO₂ ha⁻¹ for a dolerite; Lefebvre et al., 2019), very large land areas are required, carrying carbon costs associated with the logistics of transport and spreading. In contrast, construction of green infrastructure alongside highways and other assets provides the opportunity to include much larger volumes of rock with a more focussed carbon capture function. For example, a

* Corresponding author. School of Applied Sciences, Abertay University, United Kingdom.

E-mail address: e.jorat@abertay.ac.uk (M.E. Jorat).

<https://doi.org/10.1016/j.jenvman.2022.115016>

Received 2 January 2022; Received in revised form 29 March 2022; Accepted 2 April 2022

Available online 20 April 2022

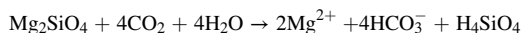
0301-4797/© 2022 The Authors. Published by Elsevier Ltd. This is an open access article under the CC BY license (<http://creativecommons.org/licenses/by/4.0/>).

constructed topsoil with the equivalent of 10 cm dolerite rock dust at 1623 kg/m^3 would use 1623 t ha^{-1} dolerite, with a CO_2 removal potential of $370 \text{ t CO}_2 \text{ ha}^{-1}$, a factor of 15 times greater than the highest application rate envisaged for agriculture. Additional CO_2 removal can be achieved by inclusion of fines from crushing demolished concrete structures into engineered soils (Washbourne et al., 2015).

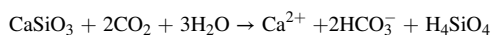
Carbon can be captured in soil in organic and inorganic form (Schlesinger, 1982). The potential of storing organic carbon is limited because soil organic matter decomposes, returning CO_2 ultimately to the atmosphere (Sommer and Bossio, 2014, Fig. 1). In contrast, once transformed to inorganic carbon, as carbonate, CO_2 becomes part of pedogenic carbonate minerals (carbonation), or the soil solution (ERW), and so is effectively removed from the biologically-driven part of the carbon cycle.

Possible sources of calcium for the formation of pedogenic carbonates include natural Ca-rich silicate rocks, such as dolerite or basalt (Beerling et al., 2020; Manning et al., 2013). In addition, Ca-rich silicates are available as waste streams, including basic steel slags and concrete derived from demolition (Renforth, 2019). The quantities available globally exceed 1 billion tonnes per year, with a carbon capture potential in excess of 100 million tonnes annually (Renforth et al., 2011b). Tangintthai et al. (2019) carried out a detailed material flow analysis for concrete-related materials produced in the UK and Thailand, demonstrating the importance of policy in optimising their management; this could include their use in carbon capture.

The process by which CO_2 is removed from the atmosphere by rock weathering has been addressed by many authors (Manning, 2008; Renforth et al., 2009; Manning et al., 2013; Beerling et al., 2020). Current understanding of the link between photosynthesis and the formation of natural pedogenic carbonates has developed as a consequence of the pioneering C and O stable isotope studies reviewed by Cerling (1984). Briefly, once CO_2 has entered the soil solution, either via rainfall (equilibration with atmospheric CO_2) or via biological processes within the soil (microbial respiration; plant root exudation etc), it reduces the pH of the aqueous phase, accelerating weathering of silicate rocks. In much of the literature, this is based on the weathering reaction for olivine (forsterite; Mg_2SiO_4):



A similar reaction can be written for the calcium silicate mineral wollastonite (CaSiO_3):



Both of these reactions summarise the weathering of the silicate minerals in a soil, which takes place at rates dependant on the mineral dissolution rate (Palandri and Kharaka, 2004) and the soil pH. Depending on the overall chemical composition of the soil solution, saturation with respect to the mineral calcite (CaCO_3) can occur if there is sufficient Ca or bicarbonate, and calcite then precipitates. In very Mg-rich materials, magnesium carbonate minerals can precipitate (e.g., McCutcheon et al., 2016). Confirmation of the pedogenic formation of

these carbonate minerals is provided by combined C and O stable isotope investigations (^{12}C , ^{13}C , ^{16}O , ^{18}O ; Cerling, 1984); the process of photosynthesis fractionates these natural isotopes to give a distinctive signature that is reserved when the carbonate mineral precipitates. This is augmented by ^{14}C dating, which shows a high proportion of modern carbon in calcite from urban soils (Washbourne et al., 2012, 2015; Jorat et al., 2015a, 2020).

Carbonate formation underestimates the amount of CO_2 removed from the atmosphere by weathering. In the process of enhanced rock weathering (ERW; Moosdorf et al., 2014), CO_2 derived from the atmosphere is consumed by rock weathering, and the total amount can be estimated from the quantities of Ca, Mg, Na and K in the rock (correcting for S and P), as explained in detail by Renforth (2019). However, ERW leaves no trace of any product within the soil, as all solutes are removed in solution (as demonstrated very elegantly by Moulton et al., 2000).

Recent research has shown that soil containing demolition waste can remove up to $85 \text{ t CO}_2 \text{ ha}^{-1}$ annually, based on measurements of soil inorganic carbon content, representing calcite, through appropriate management of brownfield sites to capture CO_2 in a form of pedogenic carbonate, and so create a stable sink (Washbourne et al., 2012, 2015; Manning and Renforth, 2013; Renforth et al., 2009; Jorat et al., 2015a). Formation of pedogenic carbonate, calcite, in soil depends on availability of calcium (Manning et al., 2013), and this is achieved through natural weathering of silicate minerals. Two important sources for silicate minerals in engineered soils are basic silicate rocks (e.g., dolerite and basalt) and artificial calcium silicate or hydroxide minerals present in concrete and cement (Jorat et al., 2015a). Importantly, for monitoring purposes pedogenic carbonate formation can be measured on soil samples by determining the soil's total inorganic carbon (TIC) content. There is no corresponding measurement that can be made to determine the rate or amount of ERW in the field.

In a recent study of 20 urban brownfield sites in north-east England, measurement of soil TIC showed that the soils had removed $59 \text{ t CO}_2 \text{ ha}^{-1}$ annually (Jorat et al., 2020). With an urban land area of 1,833, 015 ha (ONS, 2021), redevelopment and construction, especially of infrastructure, offers opportunities to design a carbon capture function into associated green space (for example, Highways England manages 25,000 ha of land; Highways England, 2015). However, to date, no research has been carried out to investigate changes in geotechnical properties as a result of mineral carbonation or weathering in engineered soils. In addition, detailed analysis of the capacity of engineered soils to sequester CO_2 with an authentic day-zero baseline has not been attempted. Lastly, impact of depth on calcite precipitation in engineered soils has not been assessed. Designing a function of inorganic carbon sequestration into land associated with future developments would significantly increase soil capacity to capture and store carbon and make a potentially valuable contribution to net-zero emission targets.

In this paper, we examine the potential for use of quarry fines and crushed concrete in engineered soils that might be used in infrastructure with the express purpose of CO_2 removal. We address the geotechnical behaviour of such soils, evaluate their ability to remove CO_2 , and consider the availability of such materials at scale. We focus on measuring the carbonate content of the soil, using C and O stable isotopes to demonstrate the formation of a carbonate product, calcite, in the soil. The paper describes the results of a unique experiment designed to remove atmospheric CO_2 in artificial soils plots large enough to permit testing of strength using cone penetration, and on a scale appropriate to provide information that informs geotechnical design. The experiment was designed to test the hypothesis that soil carbonation increases strength. It also demonstrates the impact of the design on drainage, with implications for run-off and flood management.

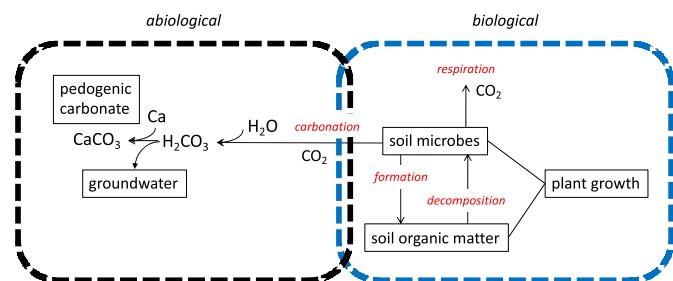


Fig. 1. Schematic representation of the biological (after Bradford, 2013) and abiological pathways for carbon in the coupled plant-soil system.

2. Materials and methods

2.1. Carbon capture experimental plots

The inorganic carbon capture experiment was constructed at Cockle Park Farm, Morpeth, north-east England (55°12'58.2"N, 1°40'58.9"W) in April 2015. At this location (owned by Newcastle University), the natural soil consists of 1.1–1.2 m of silt-size glacial till overlying sandstone. The experiment consists of 14 plots of 4 m (L) x 3 m (W) x 1 m (D) with a minimum of 2 m horizontal distance between adjacent plots (Fig. 2). Twelve of the experimental plots used crushed concrete aggregate with particle size of <4 mm (referred to concrete plot hereafter) or crushed dolerite with particle size of <4 mm (referred to dolerite plot hereafter). These sources of calcium were mixed in the following ways. In 6 plots, the calcium source was blended with a locally sourced (County Durham) Permian dune sand ('yellow sand') with spherical particle size of <2 mm. In 6 other plots, the sand was emplaced first, and overlain with a layer of the calcium source, varying thicknesses between plots (Fig. 2). In addition, two sand plots were filled only with the yellow sand. Plot composition is summarised in Fig. 2.

Plots were excavated and filled with the aggregates by a local contractor, J.O. Straughan & Co Ltd (Morpeth, UK), using a Volvo EC160CL crawler excavator. To allow maximum pore volume within the substrate and hence maximising space to accommodate inorganic carbonates, no attempt was made to compact the aggregates during the

filling operation (as suggested by Jorat et al. (2015b)). All 14 plots were covered with 0.04 m of municipal greenwaste compost to support vegetation growth, and sown with ER1F wildflower mix from Emorsgate Seeds (<https://wildseed.co.uk/mixtures/view/57>). The experimental plot area was fenced with chicken wire mesh three weeks after completion of the ground work to avoid disturbance by wild rabbit and deer. Daily rainfall data were acquired from a weather station located <200 m away from the experimental plot location. Soil temperature is recorded at the location of the weather station using temperature sensors installed at the depths of 0.1 and 0.3 m. 1 m long porous pipes were installed in all 14 experimental plots to monitor groundwater levels and capped to avoid debris falling into the pipes.

2.2. Cone penetration testing and coring

Two weeks after construction of the experimental plots, in May 2015, the first series of cone penetration tests with porewater pressure measurements (CPTu) and undisturbed cores were deployed and collected, respectively, by Electro Install Limited (Wallsend, UK). CPTu and coring operations were conducted using a Pagani TG63-150 crawler rig with 20 cm² cone area, taking 88 mm diameter cores to a depth of 1 m below ground surface to penetrate the entire depth of the plots. Cores were collected in PVC pipes and transported to a temperature controlled unit and kept at nominal 4 °C ± 1 °C (measured at 5 °C). The CPTu and coring were repeated biannually in October 2015, May and October

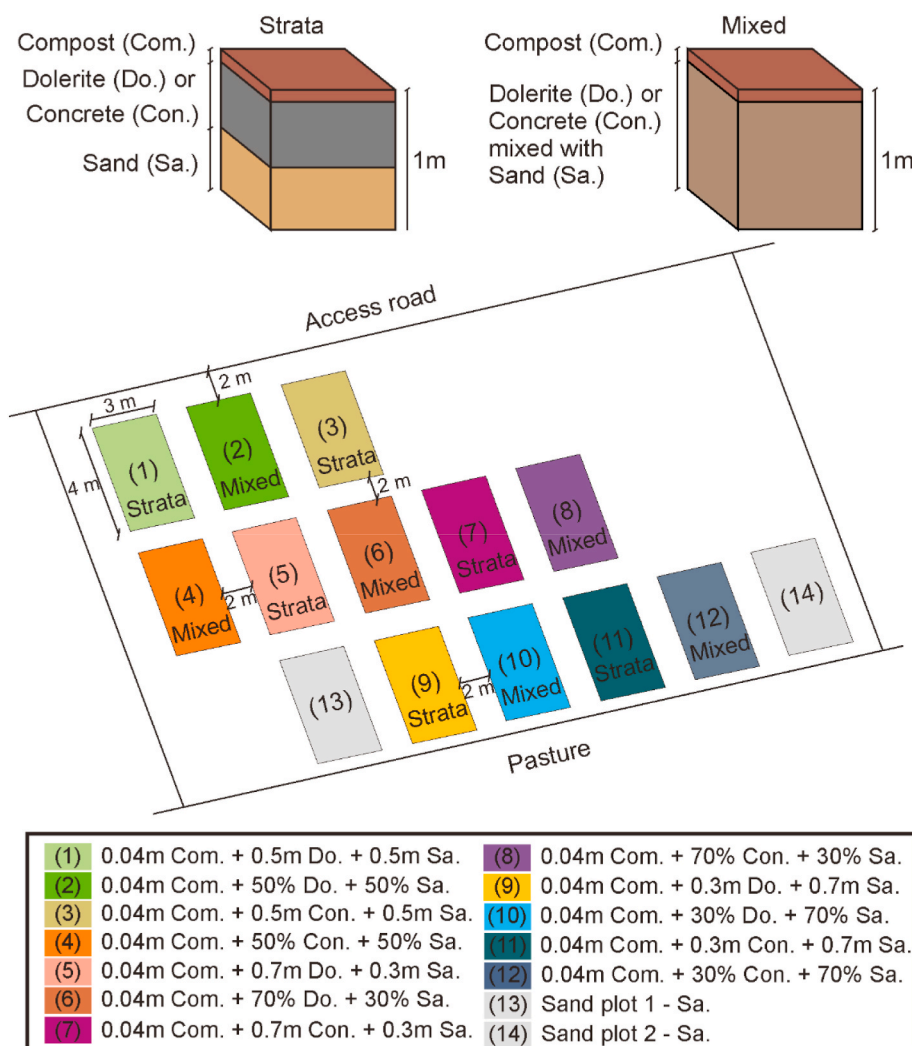


Fig. 2. Configuration of carbon capture experiment.

2016 and May 2017.

2.3. Inorganic carbon content analysis

Sub-samples were collected at selected depths from the cores collected between May 2015–17 for total inorganic carbon (TIC) content analysis, as a measure of carbonation. Firstly, to evaluate dependency of depth on TIC accumulation, samples located between 0 and 0.1 m, 0.2–0.3 m, 0.5–0.6 m, 0.7–0.8 m and 0.9–1 m were extracted from cores collected in May 2015 and May 2017 and analysed for TIC content. Secondly, to assess the relationship between CPTu tip resistance and TIC content, <100 g sub-samples were collected from the cores at a depth of 0.2 m. This depth is within the zone of maximum increase in CPTu tip resistance between May 2015–17.

To investigate dependency of TIC recorded at 0.2 m depth with soil temperature, recorded values of soil temperature at the depths of 0.1 and 0.3 m were averaged to derive calculated parameters at the depth of 0.2 m.

The collected samples were air-dried, disaggregated by hand using a pestle and mortar, and sieved in the laboratory. For TIC content analysis and variation with time (0.2 m sample depth), the <250 μm fraction was analysed by i2 Analytical Ltd. (Watford, UK) to determine inorganic carbon by acid digestion following BS 1377-3: 1990, and reported as equivalent calcium carbonate. This method provides a direct and unambiguous determination of carbonate carbon, using a commercial lab familiar with handling samples from construction sites. TIC and CO_2 equivalences were calculated stoichiometrically. In addition, to determine variation with depth, samples from plots 9–13 were analysed using a LECO (LECO Corporation, St. Joseph, MI 49085) RC612 with “Furnace Method” set to “Sample Analysis TOC” and “Method”, set to “Carbon Analysis”. Weight percentage (wt %) of carbon, total organic carbon (TOC) and total inorganic carbon (TIC) was determined directly for all samples.

2.4. C and O isotope analysis

Stable isotope data for C and O, expressed as $\delta^{13}\text{C}$ and $\delta^{18}\text{O}$ relative to Vienna Pee Dee Belemnite (VPDB), were determined by Iso-Analytical (Cheshire, U.K.) for 28 of the soil samples collected at the depth of 0.2 m in May 2015 and 2017, 8 Carboniferous Limestone and 3 Permian yellow sand samples (both to assess possible contamination by geological carbonates) and 3 samples of the crushed concrete, using a Europa Scientific 20–20 continuous-flow isotope ratio mass spectrometer (IRMS). Samples for this analysis were collected from the sub-samples corresponding to the greatest increase in CPTu tip resistance. Twelve samples were collected from the plots containing crushed concrete, twelve samples were collected from the plots containing crushed dolerite and four from the sand plot.

2.5. Data analysis

A two-way analysis of variance (ANOVA) was carried out to examine the effect of plot composition and time on TIC content. Subsequently, a *post hoc* Tukey pairwise comparison was carried out to compare the mean TIC values for each plot. All statistical work was undertaken using Minitab 17.

3. Results

3.1. Soil penetration resistance and TIC content dependency

The CPTu data show consistent increase in tip resistance values from May 2015 to 2017 (Fig. 3a). The increase is more significant in plots containing crushed dolerite compared with those containing crushed concrete. The tip resistance increase occurs for the first 0.2 m of the substrate and then reduces consistently with depth. Similar behaviour is

observed in the sand plot containing only yellow sand. Maximum tip resistance in the sand plot is similar to the maximum values observed in plots containing crushed concrete (Fig. 3a). Porewater pressure (u_2) measurements show no significant variation between May 2015 and 2017 (Fig. 3b). No groundwater table was observed inside the 1 m long porous pipes during the CPTu measurements which is consistent with further groundwater monitoring on days outside of the CPTu measurements. Well-drained aggregates in the experimental plots and local sandstone, which is weathered on its surface (at the boundary with the shallow glacial till layer), provides a drainage path for rainwater, hence no groundwater table was observed inside the porous pipes. Accordingly, no hydrostatic pressure line is included in Fig. 3b. Although porewater pressure values are small, negative measurements of porewater pressure have been observed in the plots (Fig. 3b). No markable increase in TIC content was observed between May 2015 and 2017 (Fig. 3c). Particularly, in crushed concrete and dolerite plots, loss in TIC content was observed between 0 and 0.1 m which is the zone where tip resistance values increase with depth. No consistency was observed when correlating increase in tip resistance between May 2015 and 2017 with TIC content from the same period (Fig. 3a and b).

Fig. 4 shows that TIC increased between May 2015 and 2017 at 0.2 m in all plots except one sand plot and a plot containing dolerite, which are within 1 standard error (Standard error = 0.59 (wt%)). The concrete plots accumulated more TIC compared with the dolerite plots. TIC accumulation between May 2015 and 2017 (Fig. 4) correlates with the increase in tip resistance values at the depth of 0.2 m for both dolerite and concrete plots (Fig. 3b). However, the higher TIC accumulation in concrete plots is associated with lower increase in tip resistance compared with that of dolerite plots at the depth of 0.2 m.

3.2. Variation in TIC content with season

Fig. 3 shows that plots with dolerite (plots 9 – layered and 10 – mixed) and with concrete (plot 11 – layered) consistently show an increase in TIC during the summer and autumn, whereas other plots remain similar or reduce. The concrete mix, Plot 12, shows a slight fall then an increase in TIC towards the end of the two-year period. These observations indicate differing distributions of inorganic carbon within the profile, which may relate to particulate transport or precipitation at different locations. To explore the relationships in more detail, data for cumulative rainfall and soil temperature for the month (i.e. May and October 2015, May and October 2016 and May 2017) prior to sampling have been correlated with TIC (Supplementary Information, Figure S1 and S2).

In summary, TIC increases are associated with an increase in soil temperature for the stratified concrete plot (Plot 11) and the dolerite plots (Plot 9, 10). Increase in soil temperature has no link with TIC accumulation in the sand plot (Plot 13). TIC increases with cumulative rainfall only in the concrete plot mixed with sand (Plot 12). In all other plots, TIC decreases with increasing cumulative rainfall.

3.3. Carbon and oxygen isotope data

Carbon and oxygen isotope data for concrete, dolerite and sand plots sampled in 2015 and 2017 are shown in Fig. 5, together with data for the materials used in their construction and for limestone from the vicinity of the quarry source for the dolerite. Using the approach taken by Cerling (1984) and Washbourne et al. (2015), the C and O isotope data have been plotted in the conventional plot of $\delta^{13}\text{C}$ and $\delta^{18}\text{O}$, which allows comparison of the soil samples with reference materials that could, through mixing, contribute to the observed data. Studies of pedogenic carbonates in natural soils and in urban soils (ie those that contain crushed concrete) typically show values for $\delta^{13}\text{C}$ and $\delta^{18}\text{O}$ that extend in a linear array towards increasingly negative values.

In Fig. 5, $\delta^{13}\text{C}$ and $\delta^{18}\text{O}$ values for the concrete and sand used in construction, together with values for limestone from quarries used to

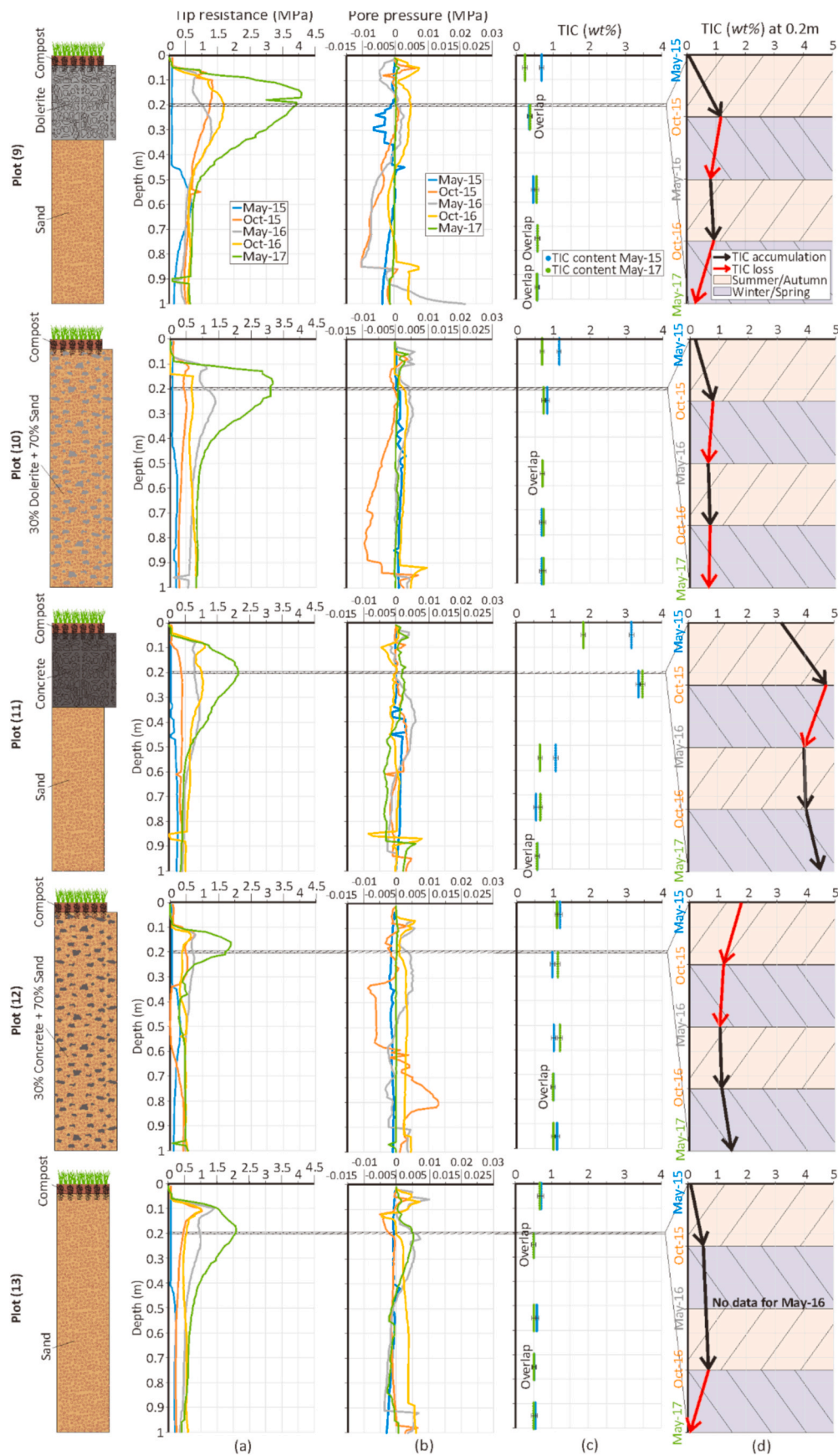


Fig. 3. Plot 9, 10, 11, 12, 13 (a) CPTu tip resistance and (b) porewater pressure, (c) total inorganic carbon content comparison between May 2015 and 2017, and (d) total inorganic carbon accumulation/loss from May 2015 to 2017 at the depth of 0.20 m.

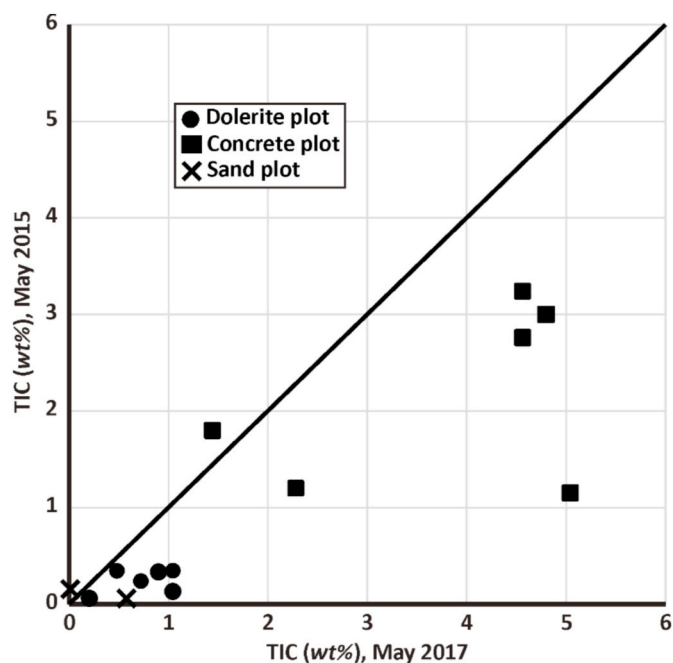


Fig. 4. TIC between May 2015 and 2017 at the depth of 0.2 m. Standard error = 0.59 (wt%).

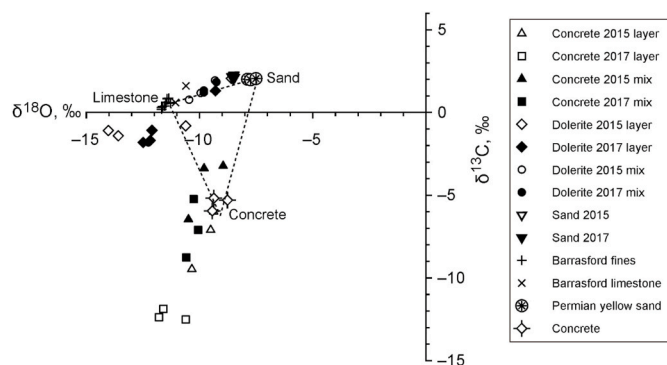


Fig. 5. C and O stable isotope data for plots and potential mixing components (sand, limestone and concrete), expressed as $\delta^{13}\text{C}$ and $\delta^{18}\text{O}$ relative to v-PDB. Barrasford refers to the quarry source used to supply the dolerite, 'Barrasford fines' representing an aged dolerite-limestone-compost mix.

source the dolerite, are shown as corners of a triangle. Values for the plots that contained crushed concrete (upward triangles and squares) show an array extending to more negative values of $\delta^{13}\text{C}$ than measured for the concrete at the start of the experiment, and there is an overall trend to more negative values with time. The plots with dolerite also show differences (diamonds and circles), but with $\delta^{13}\text{C}$ values nearer to zero and so may represent mixing with the materials used to construct the plots. However, the layered dolerite plots (i.e. with a layer of dolerite on top of sand) show more negative $\delta^{13}\text{C}$ than the plots with dolerite mixed with sand. The sand plots (downward triangles) show no change, plotting close to carbonates within the sand itself. The dolerite mixed with sand lies between the plots for sand and the plots for the dolerite layers, suggesting a mixture of values from each component. The limestone local to the dolerite source (crosses) shows a tight cluster of points with near zero $\delta^{13}\text{C}$.

From these data, and by analogy with other studies of pedogenic carbonates, it is clear that the C and O stable isotope values indicate that pedogenic carbonate formation has taken place in all plots with crushed concrete, and in the plots with dolerite fines as a surface layer.

Pedogenic carbonate formation may have taken place in plots with dolerite mixed with sand, but this cannot be determined from the C and O stable isotope data.

3.4. TIC accumulation

Biannual TIC measurements between May 2015 and 2017 show that dolerite plots, sampled at depths to 1 m, consistently accumulated TIC during summer and autumn and lost TIC during winter and spring (Fig. 3d). However, no consistent TIC accumulation/loss dependency with seasons was observed in concrete plots (Fig. 3d). Table 1 presents biannual TIC content data at the depth of 0.2 m which provides basis for more detailed analysis of TIC formation and loss between May 2015 and 2017. To calculate TIC accumulation during the two years, accumulation in TIC content every six months is taken into account and TIC content loss is regarded as zero. All TIC accumulations between May 2015 and 2017 are added to create total TIC accumulation (Table 1). Once inorganic carbon is formed, it will only be naturally removed by dissolution and entering surface and groundwater systems, or by migration of precipitated calcite fine particles (Zamanian et al., 2016). Therefore, when loss in TIC is observed in Table 1, this was regarded as dissolution or migration of sequestered inorganic carbon and hence the loss was disregarded. Based on the two-way ANOVA (reference to the statistical results in Supplementary material), the starting material of the plots were shown to significantly affect TIC accumulation ($p < 0.05$). Weight percentage of TIC, however, did not show a significant interaction with the passing of time ($p < 0.24$), which is likely due to the aforementioned seasonal variation in TIC content. Using the *post hoc* Tukey test, the means of the cumulative TIC values for the plots were shown to form three groups which are different from one another at 95% confidence (Table 2). The highest accumulation was shown for the stratified concrete plot (11), then the mixed concrete-sand plot (12) and the dolerite plots (9 and 10). The sand plot (13) showed the lowest accumulation.

4. Discussion

4.1. Geotechnical properties of constructed soils

The relationship between soil penetration resistance and TIC reflects changes in soil strength, which may have implications for the function as designed. Interpretation of the data needs to take into account the different styles of construction of each plot, recognising that in layered plots the CPTu probe encounters 100% dolerite or concrete at first, then the underlying sand. In mixed plots the entire meter depth is the same proportion of concrete or dolerite mixed with sand. This was noted by Son et al. (2020), who report greater amounts of arbuscular mycorrhizal fungi and glomalin-related soil protein in the layered plots for the 100% concrete or dolerite components.

In principle, mineral carbonation in soil leads to increase in soil strength which has notably been observed in research conducted on soil mineral carbonation (e.g., Jorat et al., 2020; DeJong et al., 2013) and Microbial Induced Calcite Precipitation in soil (e.g., Clarà Saracho et al., 2020; Jiang et al., 2017; Al Qabany and Soga, 2013). Jorat et al. (2020) suggest consistent increase in substrate bearing ratio at brownfield sites containing demolition waste with increase of substrate TIC content. However, although increase in CPTu tip resistance was observed in the plots between May 2015 and 2017, no corresponding increase in TIC content was detected during the same period (Fig. 3). The increase in CPTu tip resistance is believed to be related to development of the plant root system in the plots especially at shallow depth, and is consistent with visual observation from the cores of the distribution of roots, as well as greater fungal activity (Son et al., 2020). Kianimehr et al. (2019) reported an increase in unconfined compressive and shear strength in clay soils as a result of utilising recycled concrete aggregates. This change in mechanical properties usually is a result of increase in angularity of the soil and re-activation of un-reacted pozzolanic

Table 1

TIC content and accumulation eliminating biannual loss for plot 9, 10, 11, 12 and 13 at the depth of 0.20 m and carbon accumulation ha^{-1} per annum for the top 0.20 m of the plots.

Material Type	Plot no.	TIC (wt%)					Total accumulation (2 years)	Tonne C ha^{-1}
		May-15	Oct-15	May-16	Oct-16	May-17		Annual removal
0.70 Sand +0.30 Dolerite (Strata)	9	0.06	1.09	0.80	0.85	0.20	1.08	17.5
70% Sand +30% Dolerite (Mixed)	10	0.24	0.77	0.62	0.78	0.72	0.68	9.8
0.70 Sand +0.30 Concrete (Strata)	11	3.24	4.8	3.96	4.08	4.56	2.16	33.7
70% Sand +30% Concrete (Mixed)	12	1.8	1.19	1.03	1.14	1.44	0.41	5.8
1 m sand (Sand plot)	13	0.16	0.54	(No data)	0.72	0.01	0.56	7.6

Table 2

Tukey pairwise comparison of the mean TIC content of plots at 0.20 m depth.

Plot	N	Mean	Grouping	
0.70 Sand +0.30 Dolerite (Strata)	5	0.600	B	C
70% Sand +30% Dolerite (Mixed)	5	0.626	B	C
0.70 Sand +0.30 Concrete (Strata)	5	4.128	A	
70% Sand +30% Concrete (Mixed)	5	1.320	B	
1 m sand (Sand plot)	4	0.341		C

components remaining in recycled concrete aggregates. However, the tip resistance increase observed in concrete plots between May 2015 and 2017 is similar to the tip resistance increase observed in the sand plot only containing sand (Fig. 3). This observation dismisses the influence of crushed concrete on increasing tip resistance (Fig. 3b). As the plots were filled with the uncompacted aggregates, the lack of differences between CPTu tip resistance of concrete and sand plots could be related to insufficient interlocking of concrete and sand aggregates in concrete plots. Beerling et al. (2018) highlight the potential use of basalt (similar in chemical composition to dolerite) as agricultural input to increase productivity of soil given abundance of components such as P, K, Ca, Mg and Fe which are essential to plant growth. Accordingly, the higher increase in CPTu tip resistance observed in dolerite plots can be linked to better plant growth and improvements in the root system performance. No plant biomass measurement was conducted on the plots but visual observations of collected cores showed higher density of plant root system in dolerite plots compared with concrete plots.

From the point of view of drainage, no change in CPTu porewater pressure measurement between May 2015 and 2017 was observed (Fig. 3b). Low porewater pressure values correspond to well-drained material used in the plots, and show that two years of mineral carbonation/ERW in the specifically designed experimental plots have not resulted in reduction in drainage capacity of the substrate. Hence, the results show no evidence that there is an increased risk of flooding due to mineral carbonation in substrate during the first two years following construction in infrastructure projects that use this or similar designs. Negative porewater pressure measurements observed in the plots (Fig. 3b) could be linked to the unsaturated nature of the substrate. NRCS (2012) reported negative CPTu porewater pressure measurements in unsaturated soils resulting from suction of air bubbles created in and around the pore pressure sensor filter into the surrounding soils. This particularly is more probable in the cone's u_2 (i.e. behind the cone) pore pressure sensors, and could be the reason for the negative measurement as groundwater was never observed in the experimental plots. Researchers such as Lunne et al. (1997) have linked cavitation to negative CPTu porewater pressure measurements in dense and over-consolidated soils. However, as the experimental plots substrates are non-compacted and under-consolidated, it is unlikely that the measured negative porewater pressure values in the plots are linked to cavitation.

Higher TIC accumulation in substrates containing demolition waste (which includes crushed concrete) was observed (Jorat et al., 2020) compared with substrates containing mixtures of dolerite and compost (Manning et al., 2013), which is consistent with TIC accumulation in the plots at a depth of 0.20 m observed in Fig. 4. The sand plot accumulation

of TIC between May 2015 and 2017 at the depth of 0.20 m (Fig. 4) can be related to migration of calcite fines (geological and/or pedogenic) within the plot. Casas et al. (2019, 2020) observed dissolution of calcite when flushing water through a dolerite layer and Manning and Renforth (2013) described removal of calcite in soils with substantial drainage. Apart from the calcium source present in the dolerite and concrete plots, and given the local substrate stratigraphy consisting of glacial till overlaying a sandstone bedrock, there is no other source of calcium in vicinity of the plot location to result in precipitation of calcite in sand plots. In addition, the initial near zero TIC content at the depth of 0.20 m in sand plot in May 2015 shows the sand did not contain significant geological calcite when plots were constructed (Fig. 3d). Apart from Plot 12, increase in rainfall resulted in reduction of TIC values which could further support the migration of precipitated calcite.

4.2. Carbon and oxygen isotopes

The isotope data show that $\delta^{18}\text{O}$ and $\delta^{13}\text{C}$ in concrete, especially the layered concrete, and dolerite have become more negative between May 2015 and 2017. This is consistent with the formation of carbonate from a pathway that involves photosynthesis (Fig. 5; Cerling, 1984). The sand plot shows no change in either $\delta^{18}\text{O}$ and $\delta^{13}\text{C}$ from May 2015 and 2017, suggesting that no pedogenic carbonates were formed in this plot. There is some evidence of mixing of the carbonate between the sand and the dolerite when the plot is mixed, but as the layered dolerite shows distinctively low, negative, $\delta^{13}\text{C}$ values compared with the sand, the formation of pedogenic carbonates is evident. The differing performance of the layered and mixed construction styles relates to the nature of the sample; irrespective of the thickness of the layer, the samples reported here relate to solely dolerite or concrete, whereas in the mixed construction style these materials are diluted by the sand. This relationship has been noted by Son et al. (2020), who noted similar patterns in the distribution of arbuscular mycorrhizal fungi and glomalin-related soil protein.

4.3. TIC accumulation

TIC measurements in May 2015 and 2017 for the top 0.10 m of the plots, show reduction or no change in TIC content (Fig. 3c), however, the biannual TIC content analysis at the depth of 0.20 m shows a pattern of TIC accumulation and loss which could not be detected when TIC measurements at an interval of two years are considered (Table 1). Temperature controls the kinetics of mineral carbonation reactions and an increase in temperature is known to increase reaction kinetics (Pasquier et al., 2014). Accordingly, in warmer seasons, higher mineral carbonation is expected (although the effects may be small). Dolerite plots follow the pattern and accumulate TIC during summer/autumn, losing TIC during winter/spring (Fig. 3d). This is also consistent with increase in TIC with an increase in soil temperature observed in dolerite plots presented in (Supplementary Information, Figure S1 and S2). Casas et al. (2019) observed a large initial release of calcium from dolerite in batch reactors, which reduced significantly with increased number of solution replacements. This could explain the dolerite plots' accumulation of TIC during the first six-month period. The inconsistent

annual TIC accumulation and loss in concrete plots (Fig. 3d) was also observed in annual TIC measurement in a brownfield site containing demolition waste (Jorat et al., 2020). Demolition waste often contains geological carbonate (limestone) which could explain the inconsistent TIC values recorded in concrete plots. Inconsistent correlation between TIC values and soil temperature was also observed in concrete plots. Observing no significant variation in TIC between May 2015 and 2017 along 0–0.1 m, 0.2–0.3 m, 0.5–0.6 m, 0.7–0.8 m and 0.9–1 m could be mainly related to missing TIC data at the respective depth across the two years when the measurements were not made.

To compare with other studies, measured TIC (wt%) has been recalculated as the equivalent $t\ C\ ha^{-1}$, to a depth of 0.2 m depth. Calculating biannual TIC accumulation shows carbon sequestration of the plots is significantly above reported numbers for similar substrates. Manning et al. (2013) recorded accumulation of $4.8\ t\ C\ ha^{-1}$ annually in a 0.30 m layer consisting of 50% dolerite and 50% compost. The top 0.30 m of Plot 9 consists of dolerite and hence the sampling point of 0.20 m was within the dolerite layer. Although the depth of 0.20 m, where the TIC was measured at the plot, was located within the dolerite layer and no compost was mixed with the dolerite, the results show carbon accumulation of $17.5\ t\ C\ ha^{-1}$ annually which is nearly four times higher than the number calculated by Manning et al. (2013). Plot 10 consisting of a mixture of 30% dolerite and 70% sand shows accumulation of $9.8\ t\ C\ ha^{-1}$ annually which is twice the value calculated by Manning et al. (2013). Investigations in brownfield sites younger than five years from demolition containing crushed concrete show annual accumulation of 23 and $16\ t\ C\ ha^{-1}$, respectively (Washbourne et al., 2015; Jorat et al., 2020). The sampling point of 0.2 m at plot 11, which is within the concrete layer, shows accumulation of $33.7\ t\ C\ ha^{-1}$ annually, 1.5–2 times higher than the values reported by Jorat et al. (2020) and Washbourne et al. (2015), respectively. Plot 12 consists of a mixture of 30% concrete and 70% sand which is similar to concrete (or other silicate rich material) content in many brownfield sites, which show accumulation of $5.8\ t\ C\ ha^{-1}$ annually (Jorat et al., 2020; Washbourne et al., 2015). This value is 25% of the values recorded by Washbourne et al. (2015) and nearly 36% of the value reported by Jorat et al. (2020). Accumulation of TIC recorded at the sand plot (Table 1) is larger than the accumulation recorded for Plot 12 (mixture of 30% concrete and 70% sand) however, as the $\delta^{18}O$ and $\delta^{13}C$ signature of samples from sand plots have remained unchanged between May 2015 and 2017, we conclude that the TIC accumulation measured in sand plots resulted from migration of dissolved calcite (pedogenic and/or geological) and re-precipitation in the sand plot. This finding further enforces the deduction that a portion of precipitated calcite migrates once formed in soil. In addition, the observation highlights the importance of including migrated calcite in carbon calculation when assessing capacity of engineered soils for carbon sequestration. Results from this study indicate that calcite precipitation in soil follows a more dynamic pattern that perhaps so far has been considered. To accurately measure precipitation of calcite, an experimental lysimeter with closed boundary condition is required to fully monitor calcite content in soil and water discharge from the substrate.

4.4. Availability of materials

The potential of constructed soils to remove atmospheric CO_2 has been demonstrated in this and other studies. When considering the use of dolerite (and other basic igneous rocks) and concrete fines in construction, their availability needs to be addressed. Importantly, quarrying of basic igneous rocks for construction is well established globally, with annual production of all crushed rock estimated to be 15 billion tonnes (Sverdrup et al., 2017). What proportion of this is basalt/dolerite, however, generally is not recorded. In the UK, total crushed rock production is 130 million tonnes annually (2019; BGS 2020), of which about 40% is igneous rock, and of this it is reasonable to assume that a quarter of this is basalt or dolerite corresponding to production of the

order of 13 million tonnes per year. This figure is consistent with the production statistics given by the North East England Aggregates Working Party (2019; 2018 data)¹ and the Scottish Aggregates Survey (2015; 2012 data)², which report annual production of dolerite or basalt of 10.5 million tonnes from permitted reserves of 350 million tonnes, from the dominant producing regions within Great Britain.

About 35–40% of production of hard rock aggregate is ‘crusher fines’ produced as a consequence of the crushing process and screened to be below a nominal 4 mm grain size (Lefebvre et al., 2019). Using a figure of 25%, based on interviews with quarry managers in northern England, it is estimated that of the order of 3 million tonnes per year of material inherently suitable for incorporation into engineered soils is produced routinely in the UK, with potential CO_2 removal potential (based on $70\ kg\ t^{-1}$ for carbonation and $230\ kg\ t^{-1}$ for ERW; Lefebvre et al., 2019) of 0.2–0.69 million tonnes annually. Although a similar analysis cannot be made where mineral production statistics are lacking, the corresponding figures for the state of São Paulo, Brazil, are 1.3–2.4 million tonnes annually (Lefebvre et al., 2019). Importantly, aggregate production in the UK (and elsewhere) is managed as a strategic planning priority, to ensure supply for construction, and existing quarries typically have planning permits that extend into the 2040s, with inferred reserves extending well beyond that time. This source of material from existing industrial activities appears to be assured, with quarry fines readily available from commercial sources. As these materials are produced within an existing supply chain that sells at low cost, they are currently available at a price that is similar to other aggregate products. Although it is not possible to state a typical price, because that depends on details such as the size of the shipment amongst other factors, the United States Geological Survey gives an indicative average price for hard rock crushed aggregates of US\$12 per tonne (Willett, 2021).

The availability of crushed concrete for construction is also substantial, with the USGS estimating production of 24 million tonnes annually, compared with total crushed rock production of 1370 million (all rock types, 2017; Willett, 2021). In the UK, crushed concrete production is estimated to be around 5 million tonnes annually (Lawson et al., 2001), of which up to 1.25 million tonnes (25%) could be available as crusher fines from secondary aggregate production. It is difficult to estimate the carbon capture potential of this material given its variable composition, but analyses of recycled concrete aggregate published by Limbachiya et al. (2007) suggest CO_2 removal potential of the order of 90 (carbonation) to 250 (ERW) $kg\ t^{-1}$ of concrete, or up to 0.1–0.3 million tonnes annually from current UK arisings. The use of crusher fines from demolition involves materials with much more widely varying compositions, and the possibility of contamination from prior use needs to be assessed (Lawson et al., 2001; Bianchini et al., 2020). The costs may be greater than those associated with production of primary aggregates, given that demolition typically involves mobile plant and volumes are small compared with a quarry in a natural rock. However, the secondary aggregates industry is well developed (Lawson et al., 2001; Tangintthai et al., 2019), and costs are incurred if crusher fines need to be disposed of off-site.

On the basis of the experience gained from this experimental study, it is clear that the formation of inorganic carbonate minerals as a consequence of rock weathering cannot be fully quantified through routine sampling to 20 or 30 cm and chemical analysis. This has implications for verification of carbon dioxide removal by both natural and engineered soil. The soil system is open, allowing drainage of solutes including bicarbonate and cations, demonstrated on a catchment scale by Moulton et al. (2000). In contrast to agricultural soils, there is scope within engineered soils that form part of a construction activity to include in the

¹ Aggregate Working Parties are part of the local government planning system in England and Wales, and monitor the production in their regions of aggregates to ensure sufficient is available for construction.

² The equivalent body in Scotland is the Scottish Aggregate Survey.

design a system that allows water draining through the soil to be sampled. Analysis of the bicarbonate content of the through drainage, combined with the analysis of soil samples taken throughout the profile, allows carbon budgets to be determined with increased confidence, and permits calibration of models of inorganic carbon formation (such as CASPER; Kolosz et al., 2019).

5. Conclusions

This study has shown that construction of soils (in the geotechnical sense) using crushed dolerite and crushed concrete with sand in various combinations offers the opportunity to design a CO₂ removal function into infrastructure and other construction projects, using materials that are readily available within the existing supply chain.

The potential for CO₂ removal in the UK is currently 0.2 (carbonation) – 0.69 (ERW) million tonnes annually, using dolerite fines from existing quarries that have planning consents extending to the 2040s. Augmenting this with crusher fines from demolition of concrete structures may add a further 0.1 (carbonation) – 0.3 (ERW) million tonnes. Where statistics relating to crushed rock production are available, similar results are likely to arise in other countries.

Higher precipitation of inorganic carbon as calcite was observed in plots containing concrete compared to those containing dolerite, with the highest observed values being equivalent to 17.5 t C ha⁻¹ (Plot 9: 0.3 m dolerite and 0.7 m sand) and 33.7 t C ha⁻¹ (Plot 11: 0.3 m concrete and 0.7 m sand) annually, calculated from extrapolation of results derived from the TIC analysis. Carbon and oxygen isotope analysis show that δ¹⁸O and δ¹³C values in concrete and dolerite plots became more negative, corresponding to formation of pedogenic calcite and hence inorganic carbon sequestration.

Biannual TIC analysis shows a pattern of accumulation and loss which varies in concrete and dolerite plots. Soil temperature appears to have a significant impact on TIC values: increase in temperature predominantly resulted in TIC accumulation. Rainfall data shows TIC loss with increase in rainfall which supports pattern of TIC accumulation and loss observed in concrete and dolerite plots.

Biannual TIC measurement shows that accumulation was maximum within dolerite and concrete layer compared to plots with the materials mixed with sand.

Geotechnical properties were investigated between May 2015 and 2017. Correlation between CPTu tip resistance and substrate TIC showed that mineral carbonation had no apparent impact on penetration resistance. Mineral carbonation apparently has no negative impact on ground bearing capacity during the period of the study. In addition, CPTu porewater pressure measurements show that mineral carbonation does not result in reduction in drainage of the substrate, hence does not increase the risk of runoff which could lead to flooding.

Practical application of the results reported here for carbon capture within engineered soils aligns with existing supply chains and risk assessment protocols. Validation of claims of carbon capture need to be considered at the design stage, so that inorganic carbon entering groundwater or hydrological systems can be quantified.

Credit author statement

M. Ehsan Jorat: Conceptualization; Data curation; Formal analysis; Investigation; Methodology; Project administration; Resources; Software; Validation; Visualization; Roles/Writing - original draft; Writing - review & editing. **Karl E. Kraavi:** Data curation; Formal analysis; Investigation; Methodology; Roles/Writing - original draft. **David A. C. Manning:** Conceptualization; Data curation; Formal analysis; Funding acquisition; Methodology; Project administration; Resources; Software; Supervision; Validation; Visualization; Roles/Writing - original draft; Writing - review & editing.

Declaration of competing interest

The authors declare that they have no known competing financial interests or personal relationships that could have appeared to influence the work reported in this paper.

Acknowledgement

We acknowledge financial support from the Engineering & Physical Sciences Research Council (EP/K034952/1). We thank Mark Goddard, Kevin Stott and Chris Teasdale for their assistance in the field and in processing samples. We thank two anonymous reviewers for their constructive feedback.

Appendix A. Supplementary data

Supplementary data to this article can be found online at <https://doi.org/10.1016/j.jenvman.2022.115016>.

References

- Al Qabany, A., Soga, K., 2013. Effect of chemical treatment used in MICP on engineering properties of cemented soils. *Geotechnique* 63 (4), 331–339. <https://doi.org/10.1680/geot.SIP13.P.022>. <http://www.icevirtuallibrary.com/doi/10.1680/geot.SI13.P.022>.
- Beerling, D.J., Leake, J.R., Long, S.P., et al., 2018. Farming with crops and rocks to address global climate, food and soil security. *Nat. Plant* 4, 138–147. <https://doi.org/10.1038/s41477-018-0108-y>.
- Beerling, D.J., Kantzas, E.P., Lomas, M.R., Wade, P., Eufrazio, R.M., Renforth, P., Sarkar, B., Andrews, M.G., James, R.H., Pearce, C.R., Mercure, J.-F., Pollitt, H., Holden, P.B., Edwards, N.R., Khanna, M., Koh, L., Quegan, S., Pidgeon, N.F., Janssens, I.A., Hansen, J., Banwart, S.A., 2020. Potential for large-scale CO₂ removal via enhanced rock weathering with croplands. *Nature* 583, 242–248. <https://doi.org/10.1038/s41586-020-2448-9>.
- Bianchini, G., Ristovski, I., Milcov, I., Zupac, A., Natali, C., Salani, G.M., Marchina, C., Brombin, V., Ferraboschi, A., 2020. Chemical Characterisation of Construction and Demolition Waste in Skopje City and its Surroundings (Republic of Macedonia) Sustainability, vol. 12, p. 2055. <https://doi.org/10.3390/su12052055>.
- Bradford, M.A., 2013. Thermal Adaptation of Decomposer Communities in Warming Soils. *Front. Microbiol.* <https://doi.org/10.3389/fmicb.2013.00333>.
- Casas, C.C., Schaschke, C.J., Akunna, J.C., Jorat, M.E., 2019. Dissolution experiments on dolerite quarry fines at low liquid-to-solid ratio: a source of calcium for MICP. *Environ. Geotech.* 1–9. <https://doi.org/10.1680/jenge.19.00067>.
- Casas, C.C., Graf, A., Brüggemann, N., Jorat, M.E., 2020. Monitoring CO₂ emissions during microbially-induced calcite precipitation in sandy soil. *Front. Microbiol.* 11, 2181.
- Cerling, T.E., 1984. The stable isotopic composition of modern soil carbonate and its relationship to climate. *Earth Planet Sci. Lett.* 71 (2), 229–240. [https://doi.org/10.1016/0012-821X\(84\)90089-X](https://doi.org/10.1016/0012-821X(84)90089-X).
- Clarà Saracho, A., Haigh, S.K., Jorat, M.E., 2020. Flume study on the effects of microbial induced calcium carbonate precipitation (MICP) on the erosional behaviour of ne sand. *Geotechnique* 1, 15. <https://doi.org/10.1680/jgeot.19.P.350>.
- DeJong, J.T., Soga, K.S., Kavazanjian, E., Burns, S., van Paassen, L., Al Qabany, A., Aydilek, A., Bang, S.S., Burbank, M., Caslake, L., Chen, C.Y., Cheng, X., Chu, J., Ciurli, S., Fauriel, S., Filet, A.E., Hamdan, N., Hata, T., Inagaki, Y., Jefferis, S., Kuo, M., Laloui, L., Larrabondo, J., Manning, D.A.C., Martinez, B., Montoya, B.M., Nelson, D., Palomino, A., Renforth, P., Santamarina, J.C., Seagren, E.A., Tanyu, B., Tsesarsky, M., Weaver, T., 2013. Biogeochemical processes and geotechnical applications: progress, opportunities, and challenges. *Geotechnique* 63, 287–301, 2013.
- Friedlingstein, P., O'Sullivan, M., Jones, M.W., Andrew, R.M., Hauck, J., Olsen, A., Peters, G.P., Peters, W., Pongratz, J., Sitch, S., Le Quéré, C., Canadell, J.G., Ciais, P., Jackson, R.B., Alin, S., Aragão, L.E.O.C., Arneeth, A., Arora, V., Bates, N.R., Becker, M., Benoit-Cattin, A., Bittig, H.C., Bopp, L., Bultan, S., Chandra, N., Chevallier, F., Chini, L.P., Evans, W., Florentie, L., Forster, P.M., Gasser, T., Gehlen, M., Gilfillan, D., Gkritzalis, T., Gregor, L., Gruber, N., Harris, I., Hartung, K., Havard, V., Houghton, R.A., Ilyina, T., Jain, A.K., Joetzjer, E., Kadono, K., Kato, E., Kitidis, V., Korsbakken, J.I., Landschützer, P., Lefèvre, N., Lenton, A., Lienert, S., Liu, Z., Lombardozi, D., Marland, G., Metz, N., Munro, D.R., Nabel, J.E.M.S., Nakaoka, S.-I., Niwa, Y., O'Brien, K., Ono, T., Palmer, P.I., Pierrot, D., Poulter, B., Resplandy, L., Robertson, E., Rödenbeck, C., Schwinger, J., Séférian, R., Skjelvan, I., Smith, A.J.P., Sutton, A.J., Tanhua, T., Tans, P.P., Tian, H., Tilbrook, B., van der Werf, G., Vuichard, N., Walker, A.P., Wanninkhof, R., Watson, A.J., Willis, D., Wiltshire, A.J., Yuan, W., Yue, X., Zaehle, S., 2020. Global carbon budget 2020. *Earth Syst. Sci. Data* 12, 3269–3340. <https://doi.org/10.5194/essd-12-3269-2020>.
- Haque, F., Santos, R.M., Chiang, Y.W., 2020. CO₂ sequestration by wollastonite-amended agricultural soils – an Ontario field study. *Int. J. Greenh. Gas Control* 97, 103017. <https://doi.org/10.1016/j.jggc.2020.103017>. ISSN 1750-5836.

- Haque, F., Santos, R.M., Chiang, Y.W., 2021. Urban farming with enhanced rock weathering as a prospective climate stabilization wedge. *Environ. Sci. Technol.* 55 (20), 13575–13578. <https://doi.org/10.1021/acs.est.1c04111>.
- Highways England, 2015, 23/6/21. https://assets.publishing.service.gov.uk/government/uploads/system/uploads/attachment_data/file/441300/N150146_-_Highways_England_Biodiversity_Plan31o.pdf.
- Jiang, N.-J., Soga, K., Kuo, M., 2017. Microbially induced carbonate precipitation (MICP) for seepage-induced internal erosion control in sand-clay mixtures. *J. Geotech. Geoenviron. Eng.* 143, 4016100. [https://doi.org/10.1061/\(ASCE\)GT.1943-5606.0001559](https://doi.org/10.1061/(ASCE)GT.1943-5606.0001559).
- Jorat, M.E., Goddard, M.A., Kolosz, B.W., Sohi, S., Manning, D.A.C., 2015a. Sustainable Urban Carbon Capture: Engineering Soils for Climate Change (SUCCESS). 16th European Conference on Soil Mechanics and Geotechnical Engineering (XVI ECSMGE 2015) (Edinburgh, United Kingdom).
- Jorat, M.E., Kolosz, B.W., Sohi, S., Lopez-Capel, E., Manning, D.A.C., 2015b. Changes in Geotechnical Properties of Urban Soils during Carbonation. In: 15th Pan-American Conference on Soil Mechanics and Geotechnical Engineering. Buenos Aires, Argentina, pp. 912–918, 2015.
- Jorat, M.E., Goddard, M.A., Manning, P., Lau, H.K., Ngeow, S., Sohi, S.P., Manning, D.A.C., 2020. Passive CO₂ removal in urban soils: evidence from brownfield sites. *Sci. Total Environ.* 703, 135573. <https://doi.org/10.1016/j.scitotenv.2019.135573>.
- Kelland, M.E., Wade, P.W., Lewis, A.L., Taylor, L.L., Sarkar, B., Andrews, M.G., Lomas, M.R., Cotton, T.E.A., Kemp, S.J., James, R.H., Pearce, C.R., Hartley, S.E., Hodson, M.E., Leake, J.R., Banwart, S.A., Beerling, D.J., 2020. Increased yield and CO₂ sequestration potential with the C4 cereal Sorghum bicolor cultivated in basaltic rock dust-amended agricultural soil. *Global Change Biol.* 26, 3658–3676.
- Khalidy, R., Haque, F., Chiang, Y.W., Santos, R.M., 2021. Monitoring pedogenic inorganic carbon accumulation due to weathering of amended silicate minerals in agricultural soils. *JoVE* 172, e61996. <https://doi.org/10.3791/61996>.
- Kianimehr, M., Tabatabaie Shourijeh, P., Binesh, S.M., Mohammadinia, A., Arulrajah, A., 2019. Utilization of recycled concrete aggregates for light-stabilization of clay soils. *Construct. Build. Mater.* 227, 116792. <https://doi.org/10.1016/j.conbuildmat.2019.116792>. ISSN 0950-0618. <https://www.sciencedirect.com/science/article/pii/S0950061819322226>.
- Kolosz, B.W., Sohi, S., Manning, D.A.C., 2019. CASPER: a modelling framework to link mineral carbonation with turnover of organic matter in soil. *Comput. Geosci.* 124, 58–71. <https://doi.org/10.1016/j.cageo.2018.12.012>.
- Lawson, N., Douglas, I., Garvin, S., McGrath, C., Manning, D.A.C., Vetterlein, J., 2001. Recycling construction and demolition wastes - a UK perspective. *Environ. Manag. Health* 12, 146–157. <https://doi.org/10.1108/09566160110389898>.
- Lefebvre, D., Goglio, P., Williams, A., Manning, D.A.C., de Azevedo, A.C., Bergmann, M., Meersmans, J., Smith, P., 2019. Assessing the potential of soil carbonation and enhanced weathering through Life Cycle Assessment: a case study for Sao Paulo State, Brazil. *J. Clean. Prod.* 233, 468–481. <https://doi.org/10.1016/j.jclepro.2019.06.099>.
- Limbachiya, M.C., Marrochino, E., Koulouris, A., 2007. Chemical–mineralogical characterisation of coarse recycled concrete aggregate. *Waste Manag.* 27, 201–208. <https://doi.org/10.1016/j.wasman.2006.01.005>.
- Lunne, T., Robertson, P.K., Powell, J.J.M., 1997. Cone Penetration Testing in Geotechnical Practice. Taylor & Francis Group, London and New York.
- Manning, D.A.C., 2008. Biological enhancement of soil carbonate precipitation: passive removal of atmospheric CO₂. *Mineral. Mag.* 72, 639–649.
- Manning, D.A.C., Renforth, P., 2013. Passive sequestration of atmospheric CO₂ through coupled plant-mineral reactions in urban soils. *Environ. Sci. Technol.* 47 (1), 135–141.
- Manning, D.A.C., Renforth, P., Lopez-Capel, E., Robertson, S., Ghazireh, N., 2013. Carbonate precipitation in artificial soils produced from basaltic quarry fines and composts: an opportunity for passive carbon sequestration. *Int. J. Greenh. Gas Control* 17, 309–317.
- McCutcheon, J., Wilson, S.A., Southam, G., 2016. Microbially accelerated carbonate mineral precipitation as a strategy for in situ carbon sequestration and rehabilitation of asbestos mine sites. *Environ. Sci. Technol.* 50 (3), 1419–1427.
- Moosdorf, N., Renforth, P., Hartmann, J., 2014. Carbon dioxide efficiency of terrestrial enhanced weathering. *Environ. Sci. Technol.* 48 (9), 4809–4816. <https://doi.org/10.1021/es4052022j.pdf>.
- Moulton, K.L., West, J., Berner, R.A., 2000. Solute flux and mineral mass balance approaches to the quantification of plant effects on silicate weathering. *Am. J. Sci.* 300, 539–570, 2000.
- North East England Aggregates Working Party, 2019. Annual Aggregates Monitoring Report 2018 downloaded 4th August 2021. <https://www.northumberland.gov.uk>.
- NRCS, 2012. Chapter 11: cone penetrometer. In: National Engineering Handbook, Part 631 Engineering Geology, Natural Resources Conservation Service (NRCS). US Department of Agriculture, Washington, DC, p. 33. <https://directives.sc.gov.usda.gov/OpenNonWebContent.aspx?content=31850.wba>.
- ONS, 2021. accessed 23rd June 2021. <https://www.ons.gov.uk/economy/environmentalaccounts/bulletins/uknaturalcapital/urbanaccounts>.
- Palandri, J.L., Kharaka, Y.K., 2004. A Compilation of Rate Parameters of Water-Mineral Interaction Kinetics for Application to Geochemical Modeling. U.S. Geological Survey Open File Report 2004-1068, Menlo Park, California, USA, p. 64.
- Pasquier, L.-C., Mercier, G., Blais, J.-F., Cecchi, E., Kentish, S., 2014. Reaction mechanism for the aqueous-phase mineral carbonation of heat-activated serpentine at low temperatures and pressures in flue gas conditions. *Environ. Sci. Technol.* 48, 5163–5170.
- Renforth, P., 2019. The negative emission potential of alkaline materials. *Nat. Commun.* 10, 1401. <https://doi.org/10.1038/s41467-019-09475-5>.
- Renforth, P., Manning, D.A.C., Lopez-Capel, E., 2009. Carbonate precipitation in artificial soils as a sink for atmospheric carbon dioxide. *Appl. Geochem.* 24, 1757–1764.
- Renforth, P., Leake, J.R., Edmondson, J., Manning, D.A.C., Gaston, K.J., 2011. Designing a carbon capture function into urban soils. *Proc. ICE - Urban Des. Plan.* 164 (2), 121–128.
- Schlesinger, W.H., 1982. Carbon storage in the caliche of arid soils: a case study from Arizona. *Soil Sci.* 133, 247–255, 4.
- From Scottish Aggregates Survey, 2015. downloaded 4th August 2021. <https://www.gov.scot/publications/scottish-aggregates-survey-2012/>.
- Sommer, R., Bossio, D., 2014. Dynamics and climate change mitigation potential of soil organic carbon sequestration. *J. Environ. Manag.* 144, 83–87.
- Son, Y., Stott, K., Manning, D.A.C., Cooper, J.M., 2020. Carbon sequestration in artificial silicate soils facilitated by arbuscular mycorrhizal fungi and glomalin-related soil protein. *Eur. J. Soil Sci.* Accepted Author Manuscript. Freely available from: <https://doi.org/10.1111/ejss.13058>.
- Sverdrup, H.U., Koca, D., Schlyter, P., 2017. A simple system dynamics model for the global production rate of sand, gravel, crushed rock and stone, market prices and long-term supply embedded into the WORLD6 model. *Biophys. Econ. Resour. Qual.* 2, 8. <https://doi.org/10.1007/s41247-017-0023-2>.
- Tangtinthai, N., Heidrich, O., Manning, D.A.C., 2019. Role of policy in managing mined resources for construction in Europe and emerging economies. *J. Environ. Manag.* 236, 613–621. <https://doi.org/10.1016/j.jenvman.2018.11.141>.
- Washbourne, C.L., Renforth, P., Manning, D.A.C., 2012. Investigating carbonate formation in urban soils as a method for capture and storage of atmospheric carbon. *Sci. Total Environ.* 431, 166–175.
- Washbourne, C.L., Lopez-Capel, E., Renforth, P., Ascough, P.L., Manning, D.A.C., 2015. Rapid removal of atmospheric CO₂ by urban soils. *Environ. Sci. Technol.* 49 (9), 5434–5440.
- Willett, J.C., 2021. Stone (Crushed). United States Geological Survey Minerals Commodity Summary (downloaded 07/10/21). <https://pubs.usgs.gov/periodicals/mcs2021/mcs2021-stone-crushed.pdf>.
- Zamanian, K., Pustovoytov, K., Kuzyakov, Y., 2016. Pedogenic carbonates: forms and formation processes. *Earth Sci. Rev.* 157 (1), 17. <https://doi.org/10.1016/j.earscirev.2016.03.003>. ISSN 0012-8252.